Honors Research Projects

The Dr. Gary B. and Pamela S. Williams Honors College

Spring 2016

Modulation of Body Weight by Intestinal Flora in Orphan Nuclear Receptor SHP-/- Mice

Ryan Mifflin
University of Akron, rsm45@zips.uakron.edu

Modulation of Body Weight by Intestinal Flora in Orphan Nuclear Receptor SHP$^{-/-}$ Mice

Ryan Mifflin
2596277

Honors Research Project in Biology
3100:499
3 Credit Hours

29 April 2016

Abstract

The whole-body deletion of small heterodimer partner (SHP) in mice is associated with protection from diet-induced obesity and hepatic steatosis upon feeding of a western diet. This protection was reported to be mediated through decreases in hepatic gene expression for lipogenesis, as well as increases in gene expression for fatty acid oxidation. SHP has been known to regulate the expression of the CYP7A1 gene, encoding the rate-limiting enzyme for bile acid synthesis, thereby altering the bile acid pool. The effects of this altered bile acid profile on the gut microbiome are unknown, as some bacteria in the gut are responsible for bile acid metabolism while others are killed by the detergent effect of bile acids. This study shows that mice without SHP display a distinctly different microbiome from wild-type mice, characterized by a reduction of phylogenetic diversity and an increased abundance of the *Bacteroidetes* phylum with a proportional decrease in *Firmicutes* abundance. Cohousing mice led to increased microbiome similarity between genotypes, with a blunted reduction of phylogenetic diversity in SHP$^{-/-}$ mice. Furthermore, cohoused mice displayed reductions in the hepatic gene expression for synthesis of fatty acids, lipid droplets, and bile acids without altering fat and liver mass. These results may suggest a relationship between SHP and the microbiome in the development of diet-induced obesity but not hepatic steatosis.

Introduction

Small heterodimer partner (SHP) is an orphan nuclear hormone receptor involved in the regulation of glucose and lipid metabolism homeostasis [1]. SHP does not bind DNA due to a lack of DNA binding domains; it represses transcription through interactions with other transcription factors [1, 3]. As SHP is involved in the negative feedback regulation of bile acid synthesis, the deletion of SHP leads to increased expression of genes involved in bile acid synthesis [3]. Upon feeding of a western diet (WD) containing high fat, carbohydrate, and cholesterol, SHP$^{-/-}$ mice displayed reduced fat accumulation in the liver [1]. Protection from diet-induced obesity (DIO) is also associated with the SHP$^{-/-}$ genotype through increased energy expenditure from brown adipose tissue, and increased β-oxidation gene expression reduces the accumulation of triglyceride lipid droplets in liver cells (hepatic steatosis) [1, 5]. Hepatic steatosis is commonly associated with insulin resistance and other metabolic disorders such as DIO and type 2 diabetes [6, 7]. More than 75% of obese patients and 25% of the general

population are affected by this disorder [6, 8]. Hepatic steatosis can progress to nonalcoholic fatty liver disease when an excess of free fatty acids triggers lipotoxicity and activates inflammatory pathways, and progression to nonalcoholic steatohepatitis occurs when inflammation and fibrosis causes damage to the hepatocytes [6, 9].

The gut microbiota also plays a major role in metabolism and formation of DIO [10]. The phyla *Bacteroidetes* and *Firmicutes*, which represent over 90% of the bacterial species in both mice and humans, are partially responsible for the energy released from the diet [11]. Traditionally, lean subjects display decreased populations of *Firmicutes* and increased *Bacteroidetes*, while obese subjects display increased populations of *Firmicutes* and decreased *Bacteroidetes* with reductions in overall diversity of the microbiome [12]. Gut bacteria are also involved in the metabolism of bile acid through the deconjugation, dehydrogenation, and dehydroxylation of primary bile acids for use in anaerobic fermentation [7]. In addition to providing energy for bacterial metabolism, the metabolism of primary bile acids forms secondary bile acids with altered antibacterial properties [13, 14]. Through detergent properties, bile acids can disrupt the lipid bilayer of bacterial cell membranes and damage arrangements of nucleic acids and proteins [15]. Several *Bacteroides, Lactobacillus,* and *Bifidobacterium* species are well known for their role in deconjugation of hydrophobic primary bile acids to produce secondary bile acids with reduced antibacterial effect [15, 16]. Dehydroxylation of primary bile acids performed by members of genus *Eubacterium* and *Clostridium* produces secondary bile acids of higher hydrophobicity, which therefore increases the antibacterial effect [16]. Bacterial susceptibility to bile acid-mediated damage is widely variable depending on species and environment [13, 16].

SHP represses bile acid synthesis through its action on the liver enzymes in the cytochrome P450 family, CYP7A1 and CYP8B1 [1]. CYP7A1 hydroxylates cholesterol as the rate-limiting first enzyme for the classical pathway of bile acid synthesis, followed by CYP8B1 to produce cholic acid, a hydrophilic primary bile acid [1, 14, 17]. The hydrophobic primary bile acid, chenodeoxycholic acid, can also be produced from CYP7A1 without CYP8B1, or through CYP7B1 in an alternate pathway [17]. Mice then convert chenodeoxycholic acid to α- and β-muricholic acid to complete the synthesis process (Supp. Fig. 1) [18]. After synthesis, these primary bile acids are conjugated in mice using dietary taurine before being secreted from the liver for storage in the gallbladder [14]. Following release from the gallbladder and passage

through the intestines, intestinal enterocytes reabsorb approximately 95% of the bile acids for return to the liver using the circulatory system, where the remainder is lost into feces [15, 19]. Once returned to hepatocytes, FXR is activated and induces SHP to inhibit CYP7A1 as a negative feedback loop on bile acid synthesis [20]. SHP further inhibits cholic acid production through repression of CYP8B1, also of the classical synthesis pathway [19]. The deletion of SHP leads to increased production of hydrophilic bile acids through derepression of both CYP7A1 and CYP8B1, causing higher production of cholic acid with reduced production of both α- and β-muricholic acid [3, 20, 21].

SHP also influences hepatic expression of genes involved in *de novo* fatty acid synthesis and lipid accumulation. The transcription factor SREBP-1c activates the fatty acid synthesis pathway in response to insulin, allowing FAS downstream to build the saturated fatty acid palmitate from acetyl-CoA and malonyl-CoA [22, 23]. While these fatty acids can be used to synthesize cell membranes and other intracellular components, their abnormal accumulation inside hepatocytes can inhibit glucose uptake and lead to insulin resistance or the formation of steatosis [22, 23]. WD feeding leads to increased fatty acid synthase (Fasn) expression to produce fatty acids [24-26]. CIDEC also promotes the formation of lipid droplets from buildup of these intracellular fatty acids [24, 27]. The deletion of SHP protects from hepatic steatosis by inhibiting CIDEC activation and upregulating the gene expression of CPT1A and ACOX1, involved in the β-oxidation of fatty acids [1, 28, 29]. CPT1A facilitates transport of long-chain fatty acids into the mitochondria for β-oxidation, and ACOX1 oxidizes very long-chain fatty acids that are esterified with CoA to begin the β-oxidation process in the peroxisome [25, 30].

Previous studies have shown that the deletion of SHP increases the amount of hydrophilic bile acids in the pool, which is predicted to affect the structure of the microbiome [3, 13-15]. Therefore, 16S tag pyrosequencing was utilized to elucidate the specific effects of SHP deletion on the gut bacteria, and also to confirm the similarities in microbiome composition associated with cohousing mice. Cohousing both genotypes together alleviates the difference in diversity between genotypes, and these mice also display reduced expression of hepatic genes for β-oxidation, and synthesis of fatty acids, lipid droplets, and bile acids. Targeting the impacts of SHP gene expression will also help elucidate the impact of the SHP-dependent pathway of bile acid regulation, and perhaps even provide greater insight into other factors involved in the increased protection of SHP^{-/-} mice from DIO and hepatic steatosis [1]. The relationship of

phenotypic changes associated with alterations in the gut microbiome in mice lacking SHP is also unknown. This study shows that SHP$^{-/-}$ mice display a distinct microbiome from the wild-type genotype (WT) through alterations in the ratio of *Firmicutes* to *Bacteroidetes* with changes in phylogenetic diversity.

Materials and Methods

Mouse Studies. Separate cages consisted of a single genotype of littermates, and cohoused cages consisted of equal numbers of WT C57BL/6NHsd and SHP$^{-/-}$ mice also based on a C57BL/6NHsd background. Age-matched mice were housed in cages of four, and cohoused cages were set up immediately after weaning at three weeks of age. Cohoused cages were used to reduce microbiome-associated differences and isolate the physiological differences associated with the altered bacterial composition. All cages were housed in a temperature and light-controlled room on a 12-hour light-dark cycle (06:30 on, 18:30 off). Diet and water was available ad libitum, consisting of either laboratory chow (5001, Lab Diet, MO) for chow diet (CD) or WD consisting of high sucrose and 42% energy from saturated fats (TD.88137, Harlan Labs, IN). All mice were fed CD until WD was introduced at eight weeks of age and fed to mice for twenty-four weeks. Body weight was taken on average every seven days following WD administration. After twelve total weeks of WD, a glucose tolerance test was performed after overnight fasting. Following intraperitoneal injection of 1 g/kg glucose solution, blood glucose was checked at thirty minute intervals for two hours using a Bayer Contour Next EZ handheld blood glucose meter (Bayer HealthCare, IN). After fourteen total weeks of western diet, mouse body composition was determined using an EchoMRI machine (EchoMRI, TX). All animals were handled humanely, and all protocols were approved by the Institutional Animal Care and Use Committee at NEOMED.

Tissue Collection and Measurement of Gene Expression. Tissue collection was performed after 6 months of WD feeding. Liver samples were used for gene expression, from which total RNA was isolated using a TRIzol solution (Life Tech, NY) [31]. cDNA was synthesized from total RNA using PrimeScript RT master mix (Clontech, CA), and qPCR was run to determine mRNA levels using an Applied Biosystems Gene Amp PCR System 9700 real-time PCR machine with iTaq Universal SYBR supermix (both from BioRad, CA). GAPDH was used as an internal control, and relative expression was determined from ΔCt values normalized

to the expression of separate WT mice fed CD. Primer sequences were obtained from http://pga.mgh.harvard.edu/primerbank, and the pathway flowchart used PathVisio v3.2.1 [5].

  Gut Microbiome Profiling. Fecal samples were collected for all cages immediately before initiation of WD, and again after ten weeks of WD feeding. Mice were placed into an autoclave-sterilized cage for thirty-six hours with sterilized water and normal diet to maintain microbiome consistency. All feces was collected in a laminar flow hood, and stored at -80ºC until use. Bacterial DNA was then extracted using a Fecal DNA MiniPrep kit (Zymo Research, CA), and PCR was performed using primers targeting the V3 and V4 region of the 16S rRNA gene (Integrated DNA Technologies, IA). The primer list is found in Table 1. Pippin Prep cassettes (1.5% agarose) were used for purification and targeted DNA collection (Sage Science, MA), and purified samples were quantified via Qubit spectroscopy (Qubit Systems, ON, Canada) using a dsDNA high-sensitivity assay kit (Invitrogen-ThermoFisher, NY). Samples were sent to the Advanced Genetic Technologies Center (University of Kentucky, Lexington) for Illumina MiSeq tag pyrosequencing run on a dual-indexed, 250 base pair flowcell (Illumina, CA). Using QIIME v1.9.1, output files were demultiplexed, and operational taxonomic unit (OTU) picking was done using an open-reference algorithm [32, 33]. For samples with greater than 104,006 sequence count, beta diversity principal coordinates analysis was estimated using unweighted UniFrac and Adonis Permanova to measure significance (p-value) and an effect size (R^2) to explain variation, and rarefied alpha diversity using Faith's phylogenetic diversity (PD) whole tree analysis [2, 4]. Unless specified otherwise, a homoscedastic Student's *t*-test was used to compare two different groups, where $P < 0.05$ was considered significantly different. Values are averages ± SD unless otherwise listed.

Table 1: The list of primers used for Illumina PCR (IDT, IA)

Name	5' Illumina Adapter Sequence	Barcode Index	Pad	Linker	Gene Specific Primer 3'
Forward primers (515F-IL)					
F1)	AATGATACGGCGACCACCGAGATCTACAC	ATCGTACG	TATGGTAATT	GT	GTGCCAGCMGCCGCGGTAA
F2)	AATGATACGGCGACCACCGAGATCTACAC	ACTATCTG	TATGGTAATT	GT	GTGCCAGCMGCCGCGGTAA
F3)	AATGATACGGCGACCACCGAGATCTACAC	TAGCGAGT	TATGGTAATT	GT	GTGCCAGCMGCCGCGGTAA
F4)	AATGATACGGCGACCACCGAGATCTACAC	CTGCGTGT	TATGGTAATT	GT	GTGCCAGCMGCCGCGGTAA
F5)	AATGATACGGCGACCACCGAGATCTACAC	TCATCGAG	TATGGTAATT	GT	GTGCCAGCMGCCGCGGTAA
F6)	AATGATACGGCGACCACCGAGATCTACAC	CGTGAGTG	TATGGTAATT	GT	GTGCCAGCMGCCGCGGTAA
F7)	AATGATACGGCGACCACCGAGATCTACAC	GGATATCT	TATGGTAATT	GT	GTGCCAGCMGCCGCGGTAA
F8)	AATGATACGGCGACCACCGAGATCTACAC	GACACCGT	TATGGTAATT	GT	GTGCCAGCMGCCGCGGTAA
Reverse primers (806R-IL)					
R1)	CAAGCAGAAGACGGCATACGAGAT	AACTCTCG	AGTCAGTCAG	CC	GGACTACHVGGGTWTCTAAT
R2)	CAAGCAGAAGACGGCATACGAGAT	ACTATGTC	AGTCAGTCAG	CC	GGACTACHVGGGTWTCTAAT
R3)	CAAGCAGAAGACGGCATACGAGAT	AGTAGCGT	AGTCAGTCAG	CC	GGACTACHVGGGTWTCTAAT
R4)	CAAGCAGAAGACGGCATACGAGAT	CAGTGAGT	AGTCAGTCAG	CC	GGACTACHVGGGTWTCTAAT
R5)	CAAGCAGAAGACGGCATACGAGAT	CGTACTCA	AGTCAGTCAG	CC	GGACTACHVGGGTWTCTAAT
R6)	CAAGCAGAAGACGGCATACGAGAT	CTACGCAG	AGTCAGTCAG	CC	GGACTACHVGGGTWTCTAAT
R7)	CAAGCAGAAGACGGCATACGAGAT	GGAGACTA	AGTCAGTCAG	CC	GGACTACHVGGGTWTCTAAT
R8)	CAAGCAGAAGACGGCATACGAGAT	GTCGCTCG	AGTCAGTCAG	CC	GGACTACHVGGGTWTCTAAT

The adapter, pad, linker, and gene-specific primer sequence is common within the forward and the reverse primers. The barcode indices are used to generate a unique string for paired-end sequencing that is recognized for sorting OTU sequences [4].

Results and Discussion

Cohousing genotypes alters body weight gain. In order to explore a potential linkage between microbiome and the lean phenotype observed in SHP^{-/-} mice, this experiment cohoused WT and SHP^{-/-} mice. It was expected that the coprophagic tendencies of mice would lead to sharing of gut bacteria, and previous studies have reported complete sharing of microbiome population within four weeks [34]. Body weight from separate cages matched previous studies, as the deletion of SHP was associated with significantly reduced weight gain upon WD feeding (Fig. 1C) [1]. Cohousing led to a dramatic decrease in the protection from body weight increases (Fig. 1B & 1D) in SHP^{-/-} mice, as mice fed CD or WD displayed a nearly equalized average body weight between genotypes. This suggests the role of the gut bacteria in the protection upon SHP deletion from DIO formation.
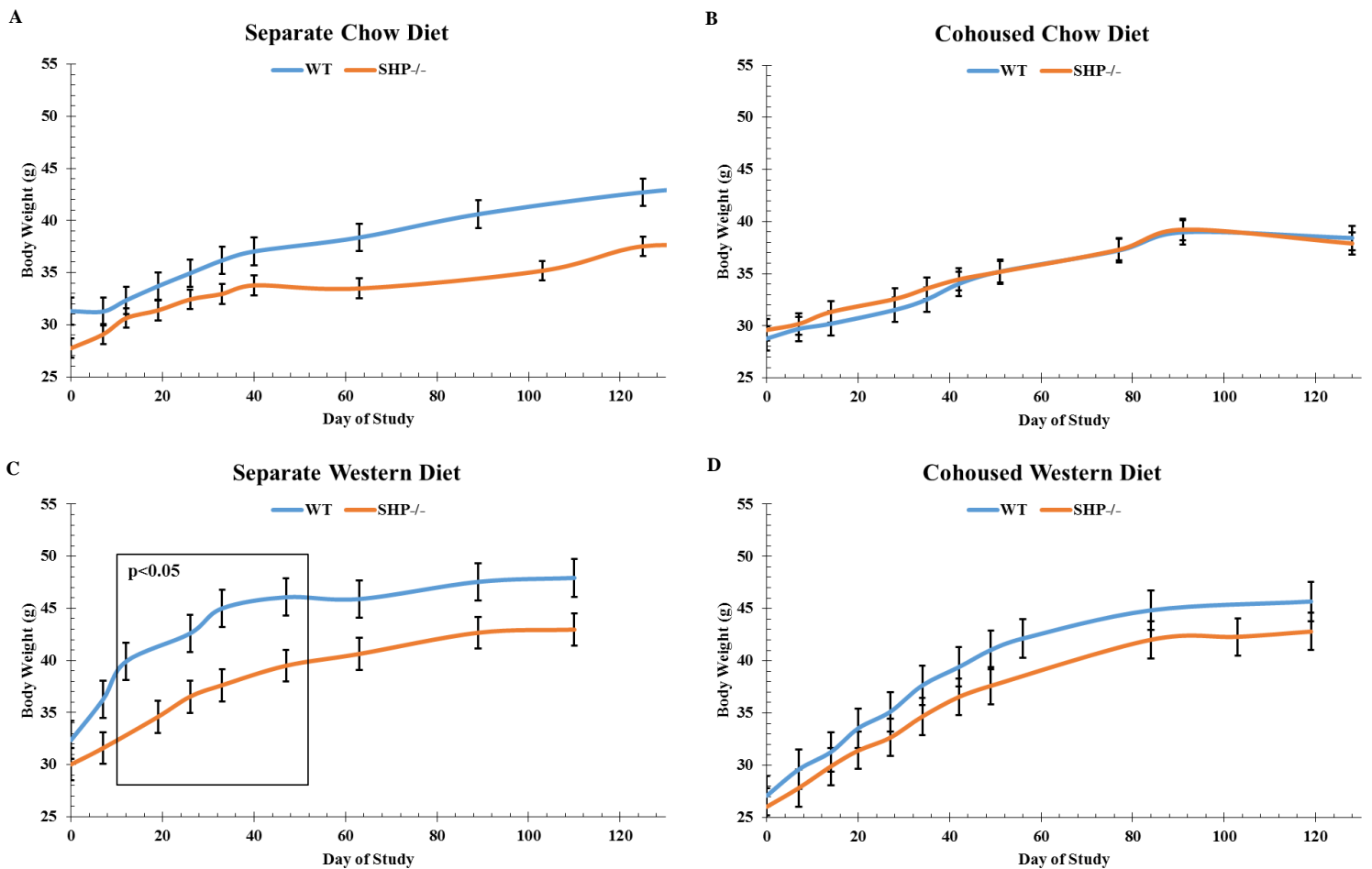
Fig. 1: Body weight changes associated with cohousing WT and SHP^{-/-} mice over the experimental period, beginning with the day WD was first administered at eight weeks of age. Values are average of total body weight per cage ± SD for each group (n=4 for all). Student's homoscedastic *t*-test was used for significance, where $P < 0.05$ was considered significant.

Deletion of SHP alters the microbiome. Sequencing of mouse feces was then performed to examine the changes in bacterial composition in the guts of both separated and cohoused animals. It was known that WD feeding and DIO led to an increase in the abundance of *Firmicutes* and a decreased abundance of *Bacteroidetes*, but the specific effect of SHP deletion on the gut microbiome was previously unknown [35]. Sequencing of the gut microbiome before and after feeding WD for 10 weeks revealed an altered bacterial composition due to diet, mouse genotype, and cohoused caging condition. Following 10 weeks of WD feeding, significantly distinct clusters of microbiome composition were seen between genotypes in separated cages (Supp. Fig. 2A). Cohousing cages alleviated these genotype-associated clusters, although significantly different clustering due to diet alterations remained (Supp. Fig. 2B). Age-associated changes in the microbiome, independent of diet, concurred with previous studies as well, as significantly distinct clusters appeared for both genotype and time (Supp. Fig. 2C & 2D) [36-38]. This suggests that diet may be a more potent influence on the microbiome than genotype.

On CD, the phylogenetic diversity of sequenced samples was not significantly different, although SHP$^{-/-}$ mice tended to display a slight reduction of diversity (Fig. 2A). However, ten weeks of WD feeding led to decreased diversity, as expected for both SHP$^{-/-}$ and WT mice (Fig. 2B) [35]. Cohoused cages display further reductions in diversity resulting from the deletion of SHP (Fig. 2C). Additionally, the deletion of SHP led to an increased diversity with CD feeding that was reversed upon WD feeding (Fig. 2B). The deletion of SHP was also linked to a reduced OTU ratio of *Firmicutes* to *Bacteroidetes*, regardless of time period or diet (Fig. 2D). One exception was seen in cohoused SHP$^{-/-}$ mice upon 10 weeks of WD feeding, which displayed a drastic increase in *Firmicutes*. This difference may reflect the increased *Firmicutes* abundance typically associated with WD feeding, although this dysbiosis was not uniform for all mice fed WD for 10 weeks [35, 39, 40]. It is hypothesized that these effects may be caused by alterations in the bile acid pool caused by the deletions of SHP and WD feeding seen in previous studies [3, 13].

A

Separate 0 Week Phylogenetic Diversity

B

Separate 10 Weeks Phylogenetic Diversity

Fig. 2: Analysis of sequencing samples (n=4 for all groups) with greater than 104,006 sequence count. Values presented are average + or – SD, where half confidence intervals are shown to increase visibility. Mice are grouped by caging-time period to compare the effects of diet alteration upon the loss of SHP. Student's homoscedastic *t*-test was used for significance: # $P < 0.05$ and ## $P < 0.01$ for diet (CD-WD), * $P < 0.05$ and ** $P < 0.01$ for genotype (WT-SHP$^{-/-}$), and ^ $P < 0.05$ for caging (separate-cohoused) significance. **(A)** Rarefied alpha diversity using Faith's PD for separate cages on CD before WD feeding began. No significance was noticed for all data sets [2]. **(B)** Faith's PD after 10 weeks of WD feeding for separate cages. **(C)** Faith's PD for cohoused cages after 10 weeks of WD feeding. **(D)** Ratio of *Firmicutes* to *Bacteroidetes*, measured by a ratio of OTU count from sequenced feces. The groups are separated by caging (Sep = Separate caging, and Co = Cohoused caging) and time length of WD feeding to compare the effects of diet alteration upon the deletion of SHP. Caging and diet are not significant ($P > 0.05$).

C

Cohoused 10 Week Phylogenetic Diversity

D

Firmicutes/Bacteroidetes Ratio

Sequencing of the microbiome composition revealed that the sum of *Firmicutes* and *Bacteroidetes* phyla account for 80-90% abundance on average, where the dominant bacteria were consistently from classes *Clostridia* and *Bacilli* of the *Firmicutes* phylum, and class *Bacteroidia* of the *Bacteroidetes* phylum (Supp. Fig. 3). Mice lacking SHP consistently displayed large increases of class *Bacteroidia* with proportional decreases in *Clostridia*, regardless of diet and length of diet. However, cohoused SHP$^{-/-}$ mice fed WD for 10 weeks

displayed a dramatic increase in *Clostridia* that reflect the large increases seen in the *Firmicutes/Bacteroidetes* ratio (Fig. 2D). However, there were several specific examples that differed from previous studies. Increases in *Erysipelotrichi* class abundance have been linked to the formation of hepatic steatosis and atherosclerosis formation, as the bacteria metabolize choline into trimethylamine, which is then converted to toxic trimethylamine N-oxide in hepatocytes and triggers cholesterol accumulation [7, 41]. In this study, only cohoused cages displayed a markedly increased abundance in the *Erysipelotrichi* class, independent of genotype and dietary alterations. Lastly, the deletion of SHP protected from increases in *Bacilli* abundance upon feeding WD, as increases are associated with the formation of DIO [38]. Further analysis of sequencing data is also required to glean further knowledge from gut bacteria changes. Sequencing after a longer period of WD feeding would show long-term effects of chronic WD feeding and complement the gene expression results [35, 37]. Phylogenetic analysis could be carried out with current data to build a tree comparing sample groups. To complement relative ratios of bacterial OTUs presented, total number of fecal bacteria should be obtained through either microscopy with fluorescent dye to target bacteria, or qPCR on the DNA extracted from fecal samples using general primers to target the 16S rRNA gene [42, 43].

Cohoused caging reduces phenotypic differences. To explore the whole-body effects associated with these microbiome changes, physiological testing was performed. As expected, $SHP^{-/-}$ mice are also protected from body fat accumulation when compared to WT mice (Fig. 3A), even on the liver (Fig. 3G) [1, 3]. However, cohoused mice displayed little differences from separated cages in their body percentage of fat and lean mass (Fig. 3A & 3B) and liver weight (Fig. 3G). This suggests that cohousing of $SHP^{-/-}$ mice was associated with loss of protection from fat accumulation but independent of formation of hepatic steatosis. Although the deletion of SHP typically results in greater glucose intolerance upon WD feeding, little difference in insulin resistance was noticed between genotype, diet, or caging following a glucose tolerance test after 3 months of WD feeding (Fig. 3C-F). However, $SHP^{-/-}$ mice in separated cages fed CD in this study displayed an abnormally increased tolerance (Fig. 3C) while no differences were noticed in cages fed WD or cohoused (Fig. 3D-F) [1]. The increased similarity in body weight with cohoused cages may be associated with the reduced genotypic difference in phylogenetic diversity (Fig. 2A-C) and principal coordinates analysis clustering (Supp. Fig. 2). The large

A **Fat % Total Body Weight**

B **Lean % Total Body Weight**

C **Separate Chow Diet**

D **Cohoused Chow Diet**

E **Separate Western Diet**

F **Cohoused Western Diet**

G **Liver Percentage**
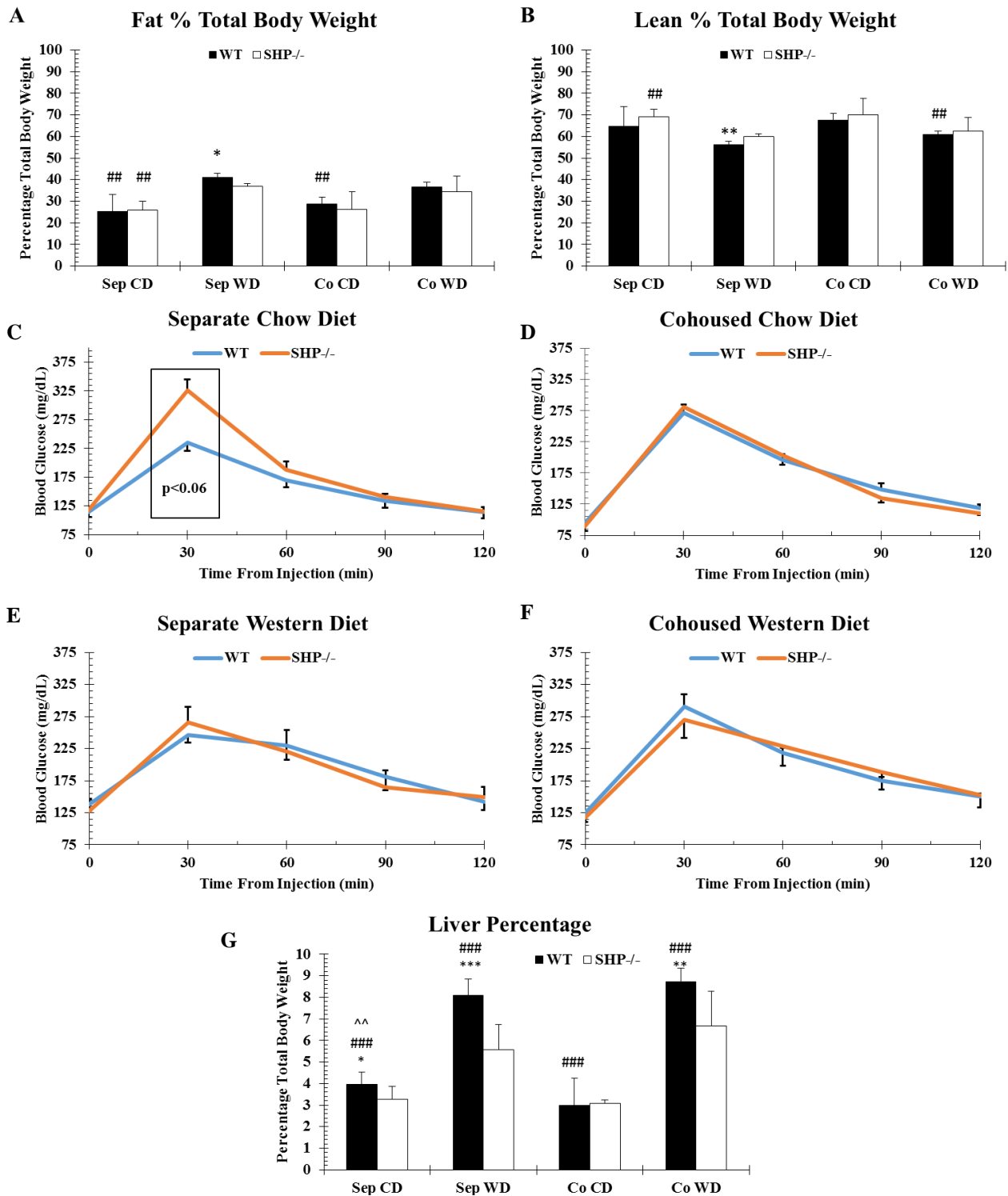
Fig. 3: Phenotype changes associated with differences in genotype over the experimental period. Each chart contains one diet and caging condition, to compare differences associated with the loss of SHP, where sample number is equal (n=4) for all groups and tests (Sep = Separate Caging, and Co = Cohoused caging). Student's homoscedastic *t*-test was used to calculate significance for all tests. # $P < 0.05$, ## $P < 0.01$, and ### $P < 0.001$ for diet (CD-WD); * $P < 0.05$, ** $P < 0.01$, and *** $P < 0.001$ for genotype (WT-SHP$^{-/-}$); ^ $P < 0.05$ and ^^ $P < 0.01$ for caging (Separate-Cohoused). **(A)** Body composition through lean and fat percentage of total body weight measured by EchoMRI after fourteen weeks of WD feeding. Values are the average ± SD. **(C, D, E, F)** Glucose tolerance test performed after twelve weeks of WD feeding via peritoneal injection of 1 g/kg glucose solution with blood glucose measurements every thirty minutes afterward. Values are average + or – SD, where half confidence intervals are shown to increase visibility between groups. **(C)** Glucose tolerance test for separate mice fed CD. **(D)** Glucose tolerance test for cohoused mice fed CD. **(E)** Glucose tolerance test for separate mice fed WD. **(F)** Glucose tolerance test for cohoused mice fed WD. **(G)** Liver weight as percent of total body weight after six months of WD feeding following tissue collection. Values are the average percent body weight ± SD.

abundance of *Firmicutes* in the cohoused SHP$^{-/-}$ mice fed WD for 10 weeks reflected the loss of protection from fat accumulation, as a large abundance of *Firmicutes* is usually seen in mice with DIO and increased body weight (Fig. 2D) [11, 35, 39]. However, cohousing buffered the loss of diversity typically seen with WD feeding, which may protect from development of DIO (Fig. 2C) [35]. Insulin resistance testing proved inconclusive, as WD feeding failed to show previously published resistance in mice lacking SHP (Fig. 3C-F) [1]. Future experiments could focus on liver triglyceride and cholesterol quantification to complement the liver size presented in this study. Hepatic lipidomics may also help explore the molecular lipid differences under each caging, genotype, and diet condition, as increased levels of ceramides and other fatty acids have been linked to the formation of insulin resistance [44-46].

Cohousing alters hepatic gene expression for β-oxidation, and fatty acid and bile acid synthesis.
Testing of hepatic gene expression was performed to determine the relationship of metabolic phenotype with alterations in the microbiome. As SHP is involved in the repression of the bile acid synthesis, enzymes for both the classical and alternate pathways were tested [3, 5]. Genes involved in β-oxidation were also tested, as the deletion of SHP protects from hepatic steatosis due to increases in β-oxidation gene expression [1, 3]. Lastly, expression of genes for the synthesis of fatty acids and the accumulation of lipid droplets was tested, as the deletion of SHP downregulates both pathways [1]. In the separate cages of this study, the deletion of SHP led to significantly increased expression of bile acid synthesis genes from both the classical and alternate pathways (Fig. 4A), and the SHP$^{-/-}$ mice displayed greater protection from fatty acid synthesis and lipid droplet formation (Fig. 4B). Surprisingly, this protection was independent of β-oxidation, as SHP$^{-/-}$ mice did not display the significantly upregulation of genes involved in β-oxidation upon WD feeding as previous studies have shown (Fig. 4C) [1]. Cohousing mice led to a generalized reduction in gene expression for bile acid, fatty acid, and lipid droplet synthesis without altering the protection associated with the loss of SHP, suggesting the shared influence of genetics and microbiome in the metabolic profile.

Contrary to previous studies, hepatic SHP gene expression was found to increase upon WD feeding (Fig. 4A) [1]. Additionally, cohousing led to increases in SHP expression, causing greater repression of CYP7A1 expression for bile acid synthesis in WT mice (Fig. 4A). Derepression by the loss of SHP leads to increased expression of the three tested bile acid

synthesis genes, CYP7A1, CYP8B1, and CYP7B1 (Fig. 4A) [1, 17]. However, cohoused mice fed WD displayed a near-zero expression of the major bile acid synthesis genes from both pathways, which will require further testing to elucidate the both the responsible mechanism and its impact on the composition of the bile acid pool. Bile acid metabolomics could also be performed in the lab of Dr. Leah Shriver (University of Akron, Department of Chemistry) to elucidate specific composition of the bile acid, especially given the drastic reductions of bile acid synthesis seen in cohoused mice fed WD (Fig. 4A).

WD feeding in separate cages led to increased expression of hepatic genes involved in synthesis of fatty acids (FAS) and formation of lipid droplets (CIDEC) for both genotypes, where the deletion of SHP protected from the significant increases seen in WT mice (Fig. 4B) [1, 44, 47]. Cohoused cages displayed reduced overall expression of both FAS and CIDEC, although the protection associated with the loss of SHP remained. The hepatic β-oxidation gene expression of CPT1A and ACOX1 (Fig. 4C) largely agreed with previous studies for separate cages [1]. However, separate WT mice fed WD displayed an abnormally high expression of ACOX1, signifying the possible dysregulation of fatty acid metabolism, as CIDEC expression is also increased. Cohoused cages display an altered expression, as WD feeding reduces the expression of both genes with the loss of protection associated to the loss of SHP (Fig. 3G). These reductions in CIDEC expression should suggest that the altered microbiome from cohousing result in reduced formation of hepatic steatosis (Fig. 4B) [24]. However, the reduced expression of fatty acid synthesis genes upon cohousing did not influence the overall liver weight, suggesting that overall levels of steatosis are unaffected (Fig. 3G).

In the future, gene expression of tissue samples from the ileum may also be used to examine genes involved with absorption of bile acid, transport into the circulatory system, and the strength of the intestinal barrier. Intestinal FAS gene expression induces *de novo* lipogenesis and promotes intestinal barrier strength, where reduced expression leads to increased leakiness that allows bacterial byproducts to enter circulation and increases cytokines involved in inflammation [41]. Bacterial byproducts absorbed into the circulatory system can activate Toll-like receptors, such as LPS activating Toll-like receptor 4, resulting in a release of cytokine proteins like IL-1β that induce inflammation [9, 48]. In the liver, IL-1β leads to the activation of TNFα, which can induce hepatic steatosis [41, 48].

A
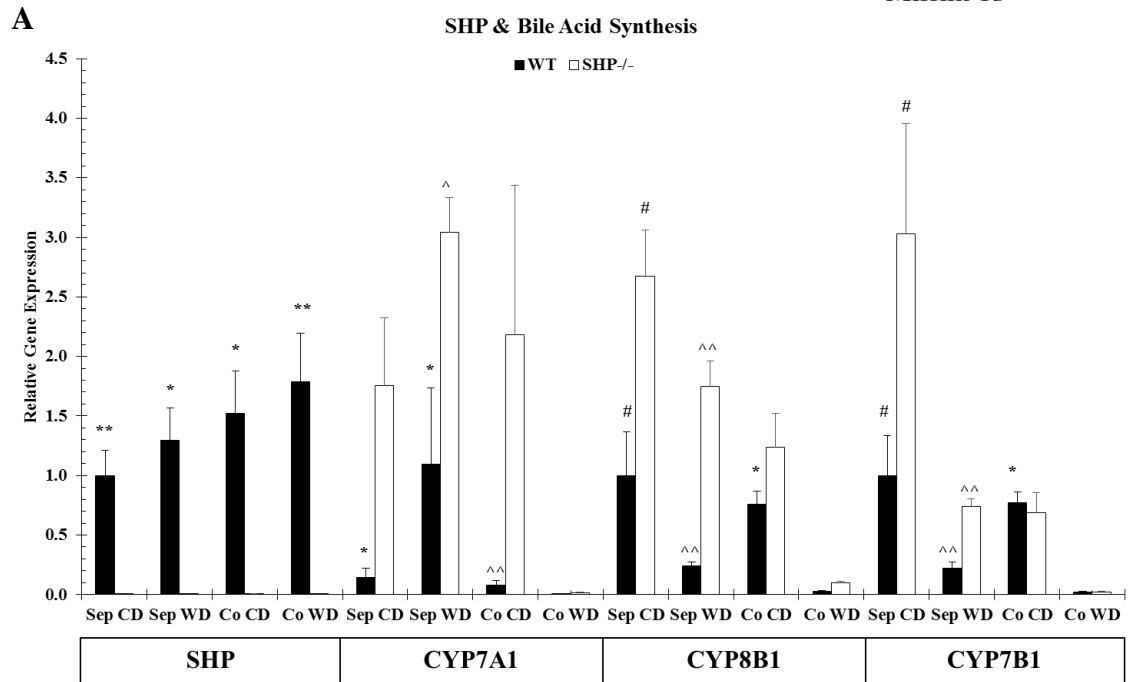
Fig. 4: Hepatic gene expression profile after six months of WD feeding. Charts are grouped (n=6 for cohoused WD cage, n=4 for all other groups) by diet and caging condition, to directly compare differences associated with SHP deletion. SHP itself was checked, as well as bile acid synthesis for the classical pathway (CYP7A1 and CYP8B1) and alternate pathway (CYP7B1). β-oxidation gene expression was checked for mitochondrial (CPT1A) and peroxisomal (ACOX1). Fatty acid synthesis gene expression was checked for palmitate synthesis (FAS) and lipid droplet accumulation (CIDEC). Values were obtained from qPCR ΔCt values with GAPDH internal control, and normalized to the expression of separate WT mice fed only CD for relative gene expression. Values are averages ± SD. Student's homoscedastic t-test was used to determine significance: # $P < 0.05$ and ## $P < 0.01$ for diet (CD-WD), * $P < 0.05$ and ** $P < 0.01$ for genotype (WT-SHP$^{-/-}$), and ^ $P < 0.05$ and ^^ $P < 0.01$ for caging (separate-cohoused).

B

C
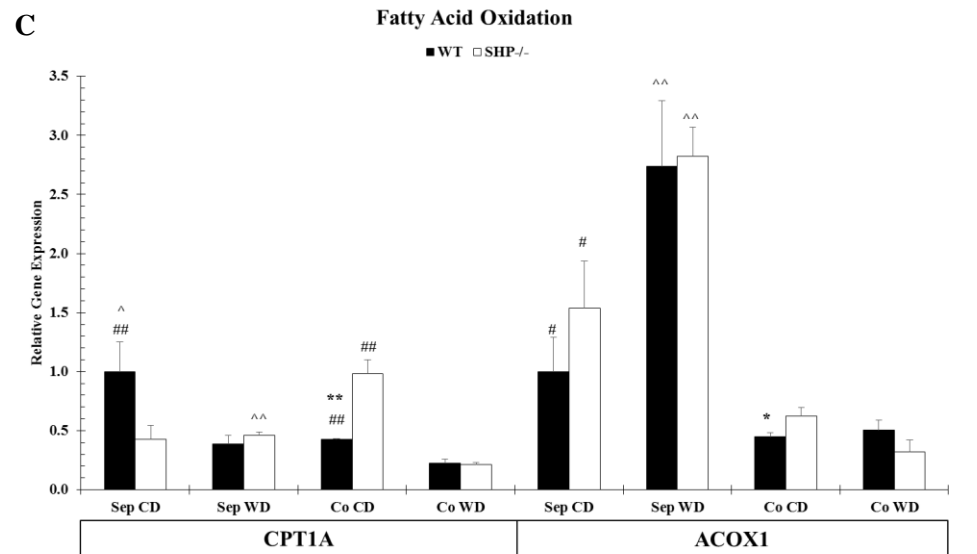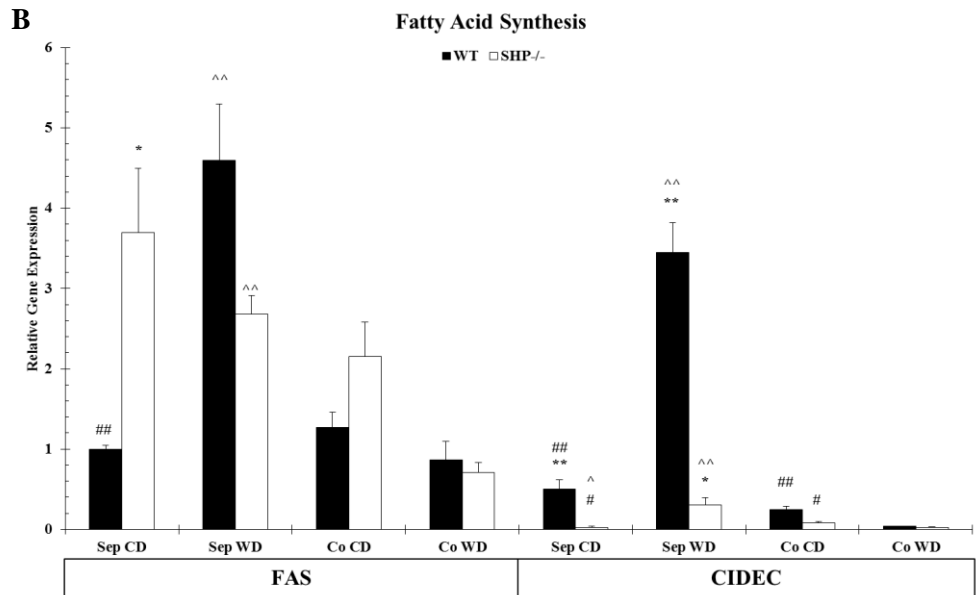
Summary. This study revealed that SHP$^{-/-}$ mice displayed a distinct microbiome from WT mice, manifested in principal coordinates analyses, a significantly reduced *Firmicutes/Bacteroidetes* ratio, and loss of phylogenetic diversity upon WD feeding. Protection from hepatic steatosis upon the deletion of SHP, seen through reduced liver percentage of total body weight, was mediated by downregulation of fatty acid synthesis and lipid droplet formation, although the expected increases in β-oxidation were not noticed. SHP$^{-/-}$ mice also displayed derepression of genes in bile acid synthesis.

Cohousing of WT and SHP$^{-/-}$ genotypes alleviated the loss of phylogenetic diversity seen in SHP$^{-/-}$ mice. The protection from DIO in SHP$^{-/-}$ mice was also reduced upon cohousing, as genotypic differences in body weight and fat accumulation were lost. However, these body weight changes were not associated with altered protection from the development of hepatic steatosis. Cohousing resulted in generalized repression of the hepatic gene expression for β-oxidation and synthesis of fatty acids, lipid droplets, and bile acids, where WD feeding caused significantly greater reductions in gene expression for bile acid synthesis. However, the effects of SHP deletion on gene expression were still present in cohoused cages, as mice lacking SHP still displayed increases in bile acid synthesis gene expression and decreases in expression of genes involved in synthesis of fatty acids and lipid droplets.

In conclusion, this study revealed that the protection from DIO and hepatic steatosis from the deletion of SHP was associated with alterations in the gut microbiome and altered gene expression. Furthermore, cohousing WT and SHP$^{-/-}$ genotypes to equalize the gut bacteria led to decreased protection from DIO upon SHP deletion while maintaining protection from hepatic steatosis.

Acknowledgments

References

1. Park, Y.J., et al., *Dissociation of diabetes and obesity in mice lacking orphan nuclear receptor small heterodimer partner.* J Lipid Res, 2011. **52**(12): p. 2234-44.
2. Faith, D.P. and A.M. Baker, *Phylogenetic diversity (PD) and biodiversity conservation: some bioinformatics challenges.* Evol Bioinform Online, 2006. **2**: p. 121-8.
3. Park, Y.J., et al., *Loss of orphan receptor small heterodimer partner sensitizes mice to liver injury from obstructive cholestasis.* Hepatology, 2008. **47**(5): p. 1578-86.
4. Caporaso, J.G., et al., *Global patterns of 16S rRNA diversity at a depth of millions of sequences per sample.* Proc Natl Acad Sci U S A, 2011. **108 Suppl 1**: p. 4516-22.
5. Park, J.E., et al., *Enhanced ethanol catabolism in orphan nuclear receptor SHP-null mice.* Am J Physiol Gastrointest Liver Physiol, 2016: p. ajpgi 00343 2015.
6. Bechmann, L.P., et al., *Free fatty acids repress small heterodimer partner (SHP) activation and adiponectin counteracts bile acid-induced liver injury in superobese patients with nonalcoholic steatohepatitis.* Hepatology, 2013. **57**(4): p. 1394-406.
7. Nicholson, J.K., et al., *Host-gut microbiota metabolic interactions.* Science, 2012. **336**(6086): p. 1262-7.
8. Tuyama, A.C. and C.Y. Chang, *Non-alcoholic fatty liver disease.* J Diabetes, 2012. **4**(3): p. 266-80.
9. Adorini, L., M. Pruzanski, and D. Shapiro, *Farnesoid X receptor targeting to treat nonalcoholic steatohepatitis.* Drug Discov Today, 2012. **17**(17-18): p. 988-97.
10. Turnbaugh, P.J., et al., *The human microbiome project.* Nature, 2007. **449**(7164): p. 804-10.
11. Ley, R.E., et al., *Microbial ecology: human gut microbes associated with obesity.* Nature, 2006. **444**(7122): p. 1022-3.
12. Turnbaugh, P.J., et al., *An obesity-associated gut microbiome with increased capacity for energy harvest.* Nature, 2006. **444**(7122): p. 1027-31.
13. Ridlon, J.M., et al., *Bile acids and the gut microbiome.* Curr Opin Gastroenterol, 2014. **30**(3): p. 332-8.
14. Sayin, S.I., et al., *Gut microbiota regulates bile acid metabolism by reducing the levels of tauro-beta-muricholic acid, a naturally occurring FXR antagonist.* Cell Metab, 2013. **17**(2): p. 225-35.
15. Fiorucci, S. and E. Distrutti, *Bile Acid-Activated Receptors, Intestinal Microbiota, and the Treatment of Metabolic Disorders.* Trends Mol Med, 2015. **21**(11): p. 702-14.
16. Begley, M., C.G. Gahan, and C. Hill, *The interaction between bacteria and bile.* FEMS Microbiol Rev, 2005. **29**(4): p. 625-51.
17. Chiang, J.Y., *Bile acids: regulation of synthesis.* J Lipid Res, 2009. **50**(10): p. 1955-66.
18. Gardes, C., et al., *Differential regulation of bile acid and cholesterol metabolism by the farnesoid X receptor in Ldlr -/- mice versus hamsters.* J Lipid Res, 2013. **54**(5): p. 1283-99.
19. Li, T. and J.Y. Chiang, *Bile acids as metabolic regulators.* Curr Opin Gastroenterol, 2015. **31**(2): p. 159-65.
20. Goodwin, B. and S.A. Kliewer, *Nuclear receptors. I. Nuclear receptors and bile acid homeostasis.* Am J Physiol Gastrointest Liver Physiol, 2002. **282**(6): p. G926-31.
21. Wang, L., et al., *Resistance of SHP-null mice to bile acid-induced liver damage.* J Biol Chem, 2003. **278**(45): p. 44475-81.
22. Aragno, M., et al., *SREBP-1c in nonalcoholic fatty liver disease induced by Western-type high-fat diet plus fructose in rats.* Free Radic Biol Med, 2009. **47**(7): p. 1067-74.
23. Jensen-Urstad, A.P. and C.F. Semenkovich, *Fatty acid synthase and liver triglyceride metabolism: housekeeper or messenger?* Biochim Biophys Acta, 2012. **1821**(5): p. 747-53.
24. Ito, M., et al., *A novel JNK2/SREBP-1c pathway involved in insulin-induced fatty acid synthesis in human adipocytes.* J Lipid Res, 2013. **54**(6): p. 1531-40.
25. Karagianni, P. and I. Talianidis, *Transcription factor networks regulating hepatic fatty acid metabolism.* Biochim Biophys Acta, 2015. **1851**(1): p. 2-8.

26. Repa, J.J., et al., *Regulation of mouse sterol regulatory element-binding protein-1c gene (SREBP-1c) by oxysterol receptors, LXRalpha and LXRbeta.* Genes Dev, 2000. **14**(22): p. 2819-30.

27. Karbowska, J. and Z. Kochan, *Intermittent fasting up-regulates Fsp27/Cidec gene expression in white adipose tissue.* Nutrition, 2012. **28**(3): p. 294-9.

28. Kim, S.C., et al., *All-trans-retinoic acid ameliorates hepatic steatosis in mice by a novel transcriptional cascade.* Hepatology, 2014. **59**(5): p. 1750-60.

29. Martinez-Jimenez, C.P., et al., *Hepatocyte nuclear factor 4alpha coordinates a transcription factor network regulating hepatic fatty acid metabolism.* Mol Cell Biol, 2010. **30**(3): p. 565-77.

30. Chow, J.D., et al., *Genetic inhibition of hepatic acetyl-CoA carboxylase activity increases liver fat and alters global protein acetylation.* Mol Metab, 2014. **3**(4): p. 419-31.

31. Chomczynski, P., *A reagent for the single-step simultaneous isolation of RNA, DNA and proteins from cell and tissue samples.* Biotechniques, 1993. **15**(3): p. 532-4, 536-7.

32. Caporaso, J.G., et al., *QIIME allows analysis of high-throughput community sequencing data.* Nat Methods, 2010. **7**(5): p. 335-6.

33. Rideout, J.R., et al., *Subsampled open-reference clustering creates consistent, comprehensive OTU definitions and scales to billions of sequences.* PeerJ, 2014. **2**: p. e545.

34. Elinav, E., C.A. Thaiss, and R.A. Flavell, *Analysis of microbiota alterations in inflammasome-deficient mice.* Methods Mol Biol, 2013. **1040**: p. 185-94.

35. Turnbaugh, P.J., et al., *Diet-induced obesity is linked to marked but reversible alterations in the mouse distal gut microbiome.* Cell Host Microbe, 2008. **3**(4): p. 213-23.

36. Mariat, D., et al., *The Firmicutes/Bacteroidetes ratio of the human microbiota changes with age.* BMC Microbiol, 2009. **9**: p. 123.

37. Campbell, J.H., et al., *Host genetic and environmental effects on mouse intestinal microbiota.* ISME J, 2012. **6**(11): p. 2033-44.

38. Turnbaugh, P.J., et al., *The effect of diet on the human gut microbiome: a metagenomic analysis in humanized gnotobiotic mice.* Sci Transl Med, 2009. **1**(6): p. 6ra14.

39. Ley, R.E., et al., *Obesity alters gut microbial ecology.* Proc Natl Acad Sci U S A, 2005. **102**(31): p. 11070-5.

40. Serino, M., et al., *Metabolic adaptation to a high-fat diet is associated with a change in the gut microbiota.* Gut, 2012. **61**(4): p. 543-53.

41. Tremaroli, V. and F. Backhed, *Functional interactions between the gut microbiota and host metabolism.* Nature, 2012. **489**(7415): p. 242-9.

42. Vaahtovuo, J., et al., *Quantification of bacteria in human feces using 16S rRNA-hybridization, DNA-staining and flow cytometry.* J Microbiol Methods, 2005. **63**(3): p. 276-86.

43. Ott, S.J., et al., *Quantification of intestinal bacterial populations by real-time PCR with a universal primer set and minor groove binder probes: a global approach to the enteric flora.* J Clin Microbiol, 2004. **42**(6): p. 2566-72.

44. Boden, G., *Role of fatty acids in the pathogenesis of insulin resistance and NIDDM.* Diabetes, 1997. **46**(1): p. 3-10.

45. Chavez, J.A. and S.A. Summers, *A ceramide-centric view of insulin resistance.* Cell Metab, 2012. **15**(5): p. 585-94.

46. Roden, M., et al., *Mechanism of free fatty acid-induced insulin resistance in humans.* J Clin Invest, 1996. **97**(12): p. 2859-65.

47. Huang, J., et al., *Molecular characterization of the role of orphan receptor small heterodimer partner in development of fatty liver.* Hepatology, 2007. **46**(1): p. 147-57.

48. Henao-Mejia, J., et al., *Inflammasome-mediated dysbiosis regulates progression of NAFLD and obesity.* Nature, 2012. **482**(7384): p. 179-85.

49. Sundaram, S.S., et al., *Mechanisms of disease: Inborn errors of bile acid synthesis.* Nat Clin Pract Gastroenterol Hepatol, 2008. **5**(8): p. 456-68.

Supplemental Figures

Supp. Fig. 1: Simplified bile acid synthesis pathway, showing only the major proteins for each conversion, and sites of SHP inhibition. The major metabolites are shown in blue boxes/text, primary bile acids are yellow-green, major enzymes are black, and regulatory proteins to highlight the involvement of SHP in negative feedback are red. (Adapted from [17, 49]).
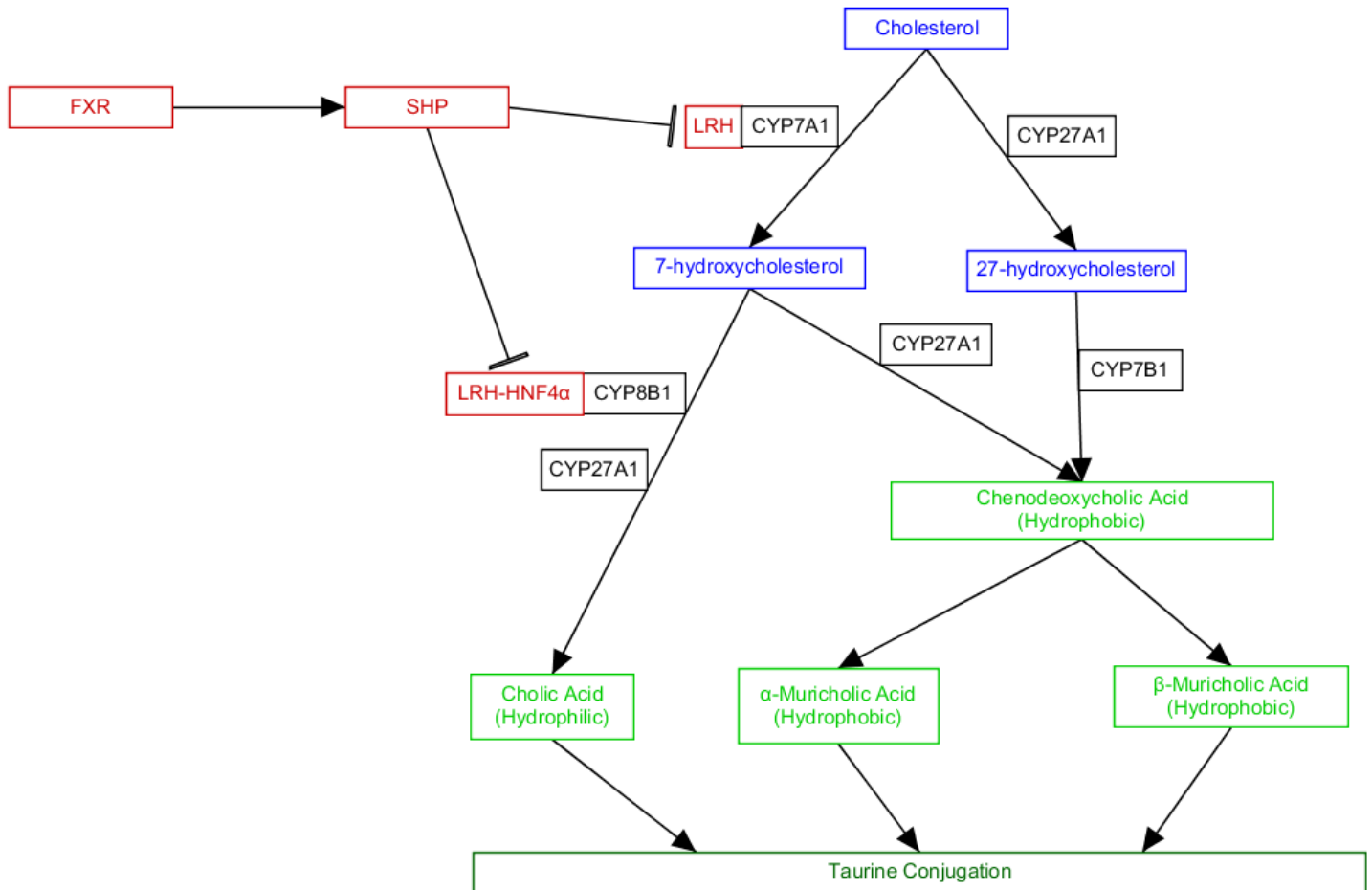
Supp. Fig. 2: Three-dimensional principal coordinates analysis plots made with QIIME using unweighted UniFrac beta-diversity data from samples with greater than 104,006 sequences each. Sample size is listed next to each color coordination for combination of genotype and diet condition. Each plot shows distinct alterations in bacterial clustering related to diet, genotype, time, and caging. Adonis Permanova was used to calculate the effect size and significance of each genotype-diet combination of samples: * $P < 0.05$ for diet (CD-WD), # $P < 0.05$ for genotype (WT-SHP$^{-/-}$), and NS is not significant ($P > 0.05$). **(A)** Separately caged mice after 10 weeks of WD, comparing the effects of genotype and diet. **(B)** Cohoused cages after 10 weeks of WD, also comparing the effects of genotype and diet. **(C)** Separately caged mice only fed CD, comparing the microbiome composition similarities between genotype and temporal changes. **(D)** Separately caged mice only fed WD, also comparing the microbiome composition similarities between genotype and temporal changes.
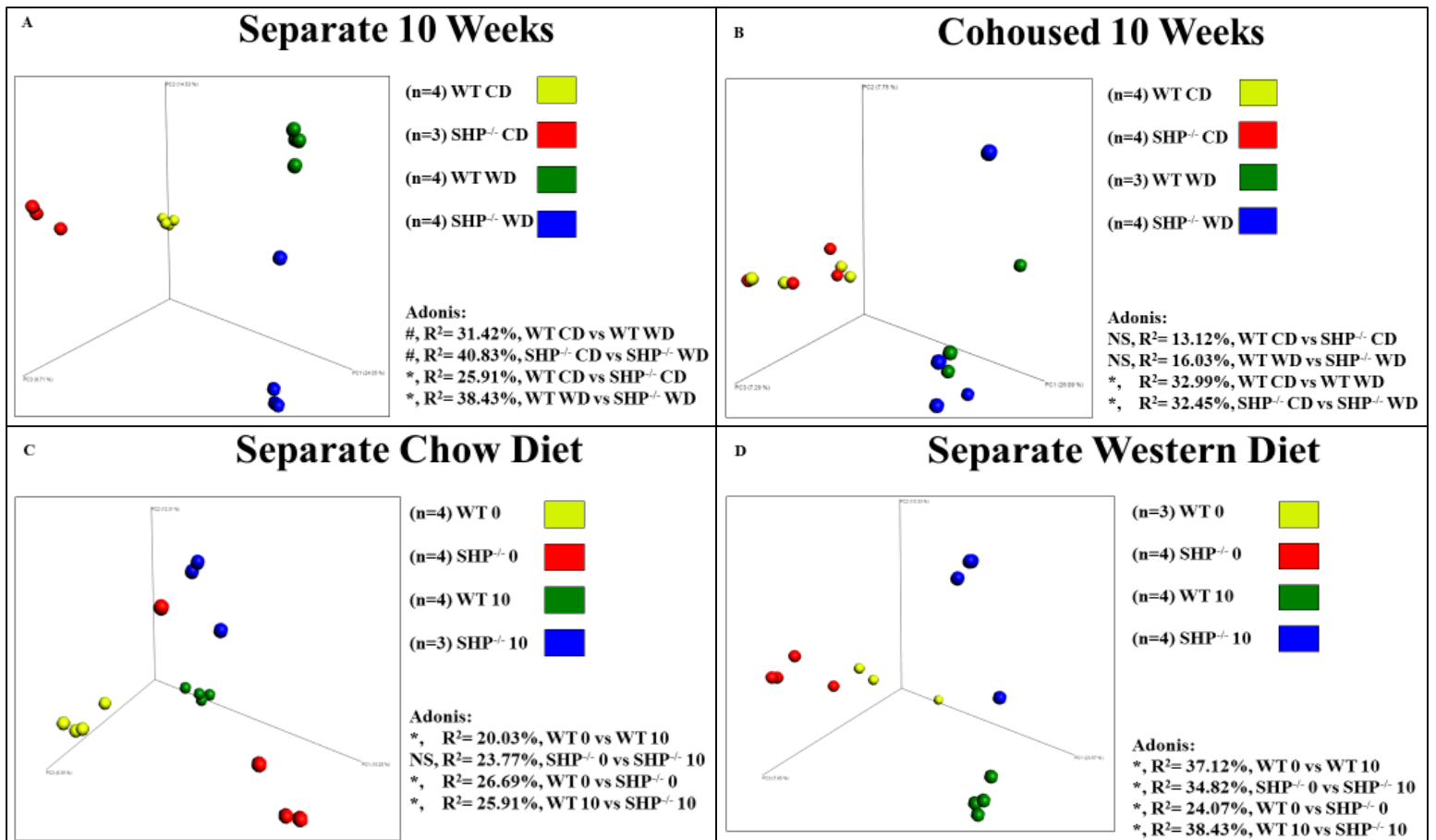
Supp. Fig. 3: Comparison of microbiome composition, via percent of class phylogeny OTU abundance. Groups (n=4 for all) are separated by caging-time period combinations to directly compare diet changes upon the loss of SHP. The bolded classes in the legend are three major classes that are consistently seen, *Clostridia, Bacilli,* and *Bacteroidia*. These classes compose at least 4.50% of the microbiome on average, seen in exact compositional abundance on the right.

Separate 0 Weeks					
Phylum	**Class**	**WT CD**	**KO CD**	**WT WD**	**KO WD**
Actinobacteria	Actinobacteria	0.00%	0.00%	0.00%	0.03%
Actinobacteria	Coriobacteriia	0.10%	0.07%	0.06%	0.11%
Bacteroidetes	Bacteroidia	38.27%	50.37%	37.87%	43.17%
Cyanobacteria	4C0d-2	0.46%	0.61%	0.79%	0.69%
Deferribacteres	Deferribacteres	0.00%	0.17%	0.38%	0.84%
Firmicutes	Bacilli	4.50%	4.93%	5.17%	4.60%
Firmicutes	Clostridia	55.76%	40.94%	53.90%	48.03%
Firmicutes	Erysipelotrichi	0.09%	0.26%	0.04%	0.03%
Proteobacteria	Alphaproteobacteria	0.04%	0.13%	0.09%	0.23%
Proteobacteria	Betaproteobacteria	0.18%	0.23%	0.12%	0.23%
Proteobacteria	Deltaproteobacteria	0.14%	0.21%	0.10%	0.29%
Proteobacteria	Epsilonproteobacteria	0.04%	0.09%	0.32%	0.45%
Proteobacteria	Gammaproteobacteria	0.00%	0.00%	0.01%	0.00%
Tenericutes	Mollicutes	0.03%	0.12%	0.94%	0.99%
Verrucomicrobia	Verrucomicrobiae	0.16%	1.23%	0.08%	0.08%
Other	Other	0.23%	0.61%	0.12%	0.20%

Separate 10 Weeks					
Phylum	**Class**	**WT CD**	**KO CD**	**WT WD**	**KO WD**
Actinobacteria	Actinobacteria	0.00%	0.00%	0.00%	0.00%
Actinobacteria	Coriobacteriia	0.08%	0.08%	0.04%	0.04%
Bacteroidetes	Bacteroidia	39.99%	44.65%	37.02%	57.49%
Cyanobacteria	4C0d-2	1.06%	0.21%	0.08%	0.09%
Deferribacteres	Deferribacteres	0.00%	0.06%	0.17%	0.34%
Firmicutes	Bacilli	3.26%	16.61%	4.29%	0.96%
Firmicutes	Clostridia	53.96%	36.87%	55.20%	38.05%
Firmicutes	Erysipelotrichi	0.08%	0.30%	0.27%	0.13%
Proteobacteria	Alphaproteobacteria	0.10%	0.04%	0.02%	0.05%
Proteobacteria	Betaproteobacteria	0.32%	0.21%	0.01%	0.02%
Proteobacteria	Deltaproteobacteria	0.13%	0.19%	2.17%	1.57%
Proteobacteria	Epsilonproteobacteria	0.10%	0.05%	0.01%	0.02%
Proteobacteria	Gammaproteobacteria	0.00%	0.00%	0.20%	0.12%
Tenericutes	Mollicutes	0.19%	0.01%	0.01%	0.00%
Verrucomicrobia	Verrucomicrobiae	0.37%	0.20%	0.26%	1.03%
Other	Other	0.34%	0.51%	0.24%	0.09%

Cohoused 10 Weeks					
Phylum	**Class**	**WT CD**	**KO CD**	**WT WD**	**KO WD**
Actinobacteria	Actinobacteria	0.00%	0.00%	0.00%	0.05%
Actinobacteria	Coriobacteriia	0.05%	0.08%	0.14%	0.10%
Bacteroidetes	Bacteroidia	42.38%	52.79%	46.94%	29.68%
Cyanobacteria	4C0d-2	0.39%	0.49%	0.31%	0.03%
Deferribacteres	Deferribacteres	0.04%	0.05%	0.10%	0.80%
Firmicutes	Bacilli	1.82%	3.70%	2.57%	0.68%
Firmicutes	Clostridia	53.60%	38.47%	46.54%	59.30%
Firmicutes	Erysipelotrichi	0.46%	0.81%	1.26%	0.52%
Proteobacteria	Alphaproteobacteria	0.06%	0.05%	0.04%	0.03%
Proteobacteria	Betaproteobacteria	0.07%	0.18%	0.01%	0.05%
Proteobacteria	Deltaproteobacteria	0.21%	0.21%	1.58%	2.93%
Proteobacteria	Epsilonproteobacteria	0.08%	0.08%	0.03%	0.04%
Proteobacteria	Gammaproteobacteria	0.00%	0.00%	0.09%	0.01%
Tenericutes	Mollicutes	0.07%	0.12%	0.00%	0.00%
Verrucomicrobia	Verrucomicrobiae	0.04%	2.01%	0.19%	5.52%
Other	Other	0.72%	0.96%	0.22%	0.26%